

The X-ray afterglow of GRB 081109A: clue to the wind bubble structure

Zhi-Ping Jin^{1,2}, Dong Xu³, Yi-Zhong Fan^{4,1}, and Da-Ming Wei¹

¹Purple Mountain Observatory, Chinese Academy of Sciences, Nanjing 210008, China

²Graduate School, Chinese Academy of Sciences, Beijing, 100012, China

³Dark Cosmology Centre, Niels Bohr Institute, University of Copenhagen, Juliane Maries Vej 30, DK-2100, Copenhagen, Denmark

⁴Niels Bohr International Academy, Niels Bohr Institute, University of Copenhagen, Blegdamsvej 17, DK-2100 Copenhagen, Denmark *

AcceptedReceived; in original form

ABSTRACT

We present the prompt BAT and afterglow XRT data of *Swift*-discovered GRB 081109A up to $\sim 5 \times 10^5$ sec after the trigger. The ground-based optical afterglow follow-ups are few for this event. The temporal and spectral indices of the X-ray afterglow emission change remarkably, which are interpreted as the GRB outflow firstly expands into the stellar wind-like medium (WIND) surrounding the progenitor (for $t \lesssim 300$ sec after the burst), and lately expands into the homogeneous interstellar medium like (ISM-like) medium. Our numerical fit of the afterglow data indicates that the parameter of the WIND medium (A_*) is ~ 0.01 , the density of the ISM-like medium is $n \sim 0.1 \text{ cm}^{-3}$, with the WIND-ISM transition radius $\sim 3.3 \times 10^{17} \text{ cm}$.

Key words: Gamma Rays: bursts –GRBs: individual (GRB 081109A)–ISM: jets and outflows–radiation mechanisms: nonthermal

1 INTRODUCTION

Gamma-ray burst (GRB) is the most luminous explosion in the Universe. It features an extremely relativistic outflow with the bulk Lorentz factor $\sim 10^2 - 10^3$ and the isotropic energy 10^{48-54} ergs. This energy is widely believed to be extracted via the core-collapse of a massive star for a conventional long(-duration) GRB (e.g., Woosley 1993) or via the merger of two compact objects for a conventional short(-duration) GRB (e.g., Eichler et al. 1989; Narayan, Paczyński, & Prian 1992). In the standard fireball model the prompt soft γ -ray emission is powered by the collision of the material shells within the relativistic outflow (i.e., the internal shocks or the internal magnetic energy dissipation); afterwards the material shells spread and merger into the one as a whole, continuing to move outwards; then the long-lived X-ray, optical, and radio afterglow emission is powered by the interaction of the overall outflow and the circum-burst medium (e.g., Piran 1999; Mészáros 2002; Zhang & Mészáros 2004). Therefore, the temporal and spectral evolution of the multi-wavelength afterglow can be a diagnose of the underlying radiation mechanism and the profile of the circum-burst medium (e.g., Sari, Piran, & Narayan 1998; Chevalier & Li 2000; Panaitescu & Kumar 2002).

For short GRBs, the circum-burst medium is expected to be of the interstellar medium (ISM) type or even of the intergalactic medium (IGM) type, for which the number density is roughly constant and much lower than unity, being consistent with the current

afterglow modeling for observed short bursts (see Nakar 2007). For most long GRBs, the afterglow modeling usually favors the ISM scenario (e.g., Panaitescu & Kumar 2002) and thus does not apparently match the collapsar model in which an ideal stellar-wind (WIND) circum-burst medium would be created. One potential solution is that the ideal WIND medium profile has been modified before the GRB explosion. As is known, massive stars are believed to enter the Wolf-Rayet stage during their late evolution and have lost a major fraction of their masses in the form of the stellar wind. The interaction between this stellar wind and the surrounding medium creates a bubble structure (e.g., Weaver et al. 1977; Wijers 2001; Ramirez-Ruiz et al. 2001; Dai & Wu 2003; Chevalier, Li, & Fransson 2004; van Marle et al. 2006, 2007). In this is the case, the WIND profile is terminated at a radius $R_t \sim 10^{18} \text{ cm}$, where the medium density jumps by a factor of four; beyond the termination radius the medium would be of ISM-like, holding up to a rather large radius $R_{\text{red}} \sim 10^{19} \text{ cm}$, where there exists a very dense ISM-like shell (i.e., the red supergiant shell) with the number density $n \sim 10^2 - 10^3 \text{ cm}^{-3}$; beyond the red supergiant shell is the remains of the the bubble structure corresponding to the progenitor activities during its main-sequence phase.

If the above picture is a good approximation for the circum-burst medium profile, it is naturally expected to find the medium transitions at $\sim R_t$ or even at $\sim R_{\text{red}}$, which are imprinted into GRB afterglow properties. In Section 2 of this work, we describe the signatures in GRB afterglows for the first transition which is more easily found and of more interest with respect to the second one. So far such a transition is possibly evident in GRB 050319

* emails: jin@pmo.ac.cn (ZPJ) and dong@astro.ku.dk (DX)

(Kamble et al. 2007) and GRB 050904 (Gendre et al. 2007) already. In Section 3, we present the X-ray afterglow observations of GRB 081109A which enable us to reach the conclusion that the WIND-ISM transition is quite clear in this event.

Throughout this work we use the notation $F(t, \nu) \propto t^\alpha \nu^\beta$ for the afterglow monochromatic flux as a function of time, where ν represents the observed frequency, α is the monochromatic flux decay index, and β is the energy index. The convention $Q_x = Q/10^x$ has been adopted in cgs units.

2 THE AFTERGLOW SIGNATURES OF THE MEDIUM TRANSITION

The GRB afterglow emission in the ISM or WIND scenarios has been extensively discussed. We use the standard fireball afterglow theory with the simple microphysical assumptions of constant energy fractions imparted to the swept-up electrons, ϵ_e , and to the generated magnetic field, ϵ_B , respectively. The characteristic frequency, ν_m , and the cooling frequency, ν_c , are due to the synchrotron radiation of the swept-up electrons. Both scenarios lead to the afterglow closure relations made of the temporal decay index α and the spectral index β , depending upon the spectral segment and the energy distribution index of $p \sim 2 - 3$ of the swept-up electrons. Usually the synchrotron self-absorption frequency, ν_a , is much lower than the optical band and thus neglected unless radio observation invoked. Therefore, with good-quality temporal and spectral data, the circum-burst medium profile can be reliably constrained. We summarize the closure relation in Table 1 apart from the $\nu < \nu_a$ cases.

For the X-ray afterglow of our interest, there are two ways to diagnose the WIND medium. (I) When $\nu_m < \nu_{\text{opt}} < \nu_c < \nu_X$ occurs, in the WIND scenario the X-ray emission drops with time as $t^{(2-3p)/4}$ while the optical emission drops faster by a factor of $1/4$. On the contrary, in the ISM scenario the optical drops more slowly than the X-ray. (II) When $\nu_m < \nu_X < \nu_c$ occurs, in the WIND scenario the X-ray emission is in the slow cooling phase and the temporal and spectral indices roughly satisfy $\alpha = (3\beta - 1)/2$.

Then how the afterglow evolves after the WIND-ISM transition at the radius R_t ? It is known that the characteristic frequency ν_m decays with time as $\propto t^{-3/2}$ in both ISM and WIND scenarios. However, the cooling frequency ν_c behaves very differently. In the WIND scenario it increases as $\propto t^{1/2}$ but in the ISM scenario it decays as $\propto t^{-1/2}$. Therefore, the following observational signatures would be evident before and after the transition. In Case I, the decay of the X-ray emission remains unchanged while the optical decay becomes shallower by a factor of $t^{1/2}$ as long as the optical band is still below ν_c . In Case II, the X-ray decay will be shallower by a factor of $t^{1/2}$ as long as the X-ray band is still below ν_c . Afterwards, when ν_c drops below the X-ray band, the X-ray decay steepens by a factor of $t^{-1/4}$. As we'll show in next Section, the X-ray afterglow of GRB 081109A well fits the Case II.

If the reverse shock optical emission is very weak, then the very early rise behavior of the optical afterglow could be an ideal probe of the density profile of the medium surrounding the progenitor. As shown in Jin & Fan (2007) and Xue et al. (2009), in the WIND scenario the very early optical rise is usually not expected to be faster than $t^{1/2}$ while in the ISM scenario the rise can be faster than t^2 . Take GRB 090102 as an example. The optical afterglow lightcurve of this burst declines as $\sim t^{-1.6}$ after the peak and then declines as $\sim t^{-0.9}$ (Klotz et al. 2009; Covino et al. 2009; Malesani et al. 2009). At the first glance the behavior may

Table 1. Temporal index α and spectral index β in the cases that the medium profile can be constrained, where the convention $F(t, \nu) \propto t^\alpha \nu^\beta$ is adopted, p is the power-law index of the swept-up electrons, and ν_a , ν_c , and ν_m are the self-absorption frequency, the cooling frequency and the characteristic frequency in the synchrotron radiation, respectively (Sari, Piran, & Narayan 1998; Chevalier & Li 2000).

Case	β	α (ISM)	α (WIND)
$\nu_a < \nu < \nu_c < \nu_m$	1/3	1/6	-2/3
$\nu_a < \nu < \nu_m < \nu_c$	1/3	1/2	0
$\max\{\nu_a, \nu_m\} < \nu < \nu_c$	$-\frac{p-1}{2}$	$\frac{3-3p}{4}$	$\frac{1-3p}{4}$
$\nu_c < \nu$	$-\frac{p}{2}$	$\frac{2-3p}{4}$	$\frac{2-3p}{4}$

be roughly consistent with the WIND-ISM transition of Case II. The initial $\sim t^3$ rise (Klotz et al. 2009), however, rules out such a possibility. We thus interpret the $\sim t^{-1.6}$ decline in the X-ray afterglow of GRB 090102 as the magnetized reverse-shock emission superposed with the forward-shock emission. In addition, the polarization observation during this period would be helpful for investigation of the emission origin.

3 THE WIND-ISM TRANSITION IN GRB 081109A

3.1 Observation and data reduction of GRB 081109A

GRB 081109A was triggered and located by the Burst Alert Telescope (BAT) onboard *Swift* at 07:02:06 UT (trigger number 334112), November 9th, 2008 (see Immler et al. 2008). We downloaded the raw data from the UK *Swift* data archive and processed them in a standard way with HEASoft 6.6. The BAT lightcurve in the 15-350 keV band was processed with the `batgrbproduct` task. This burst has a T_{90} of 61.1 ± 24.7 s in 15-1350 keV, reliably classified as a long GRB. The duration value is consistent with the duration measurement of 45 s in 8-1000 keV by the Gamma-ray Burst Monitor (GBM) onboard *Fermi* (see von Kienlin et al. 2008). The time-averaged GBM spectrum is best fitted by a power-law function with an exponential high energy cutoff. The power law index is -1.28 ± 0.09 and the cutoff energy, parameterized as E_p is 240 ± 60 keV ($\chi^2 = 510$ for 478 d.o.f.). In Fig. 1 we show the prompt lightcurves of GRB 081109A in the 15-25, 25-50, 50-100 keV bands with 1 s time binning. Spectral lag between different energy bands cannot be well measured for this event due to relatively low signal-to-noise.

The *Swift* X-ray Telescope (XRT) observations began at 65.6 seconds after the BAT trigger and discovered a bright and fading X-ray afterglow. Observations continued during the following days in several return visits, with the Windowed Timing (WT) mode for ~ 300 s after the trigger and the Photon Counting (PC) mode afterwards. Throughout the X-ray observation, spectral softening is evident. There is no need for pile-up correction to the WT data as the observed highest count rate is less than the threshold of ~ 150 count s^{-1} for WT data, but such correction is applied to early PC data when the count rate is higher than the threshold of ~ 0.6 count s^{-1} for PC data in order to get correct X-ray lightcurve and spectra. We made this correction by fitting a King function profile to the point spread function (PSF) to determine the radial point at which the measured PSF deviates from the model. The counts were extracted using an annular aperture that excluded the affected ~ 4 pixel core of the PSF, and the count rate was corrected according

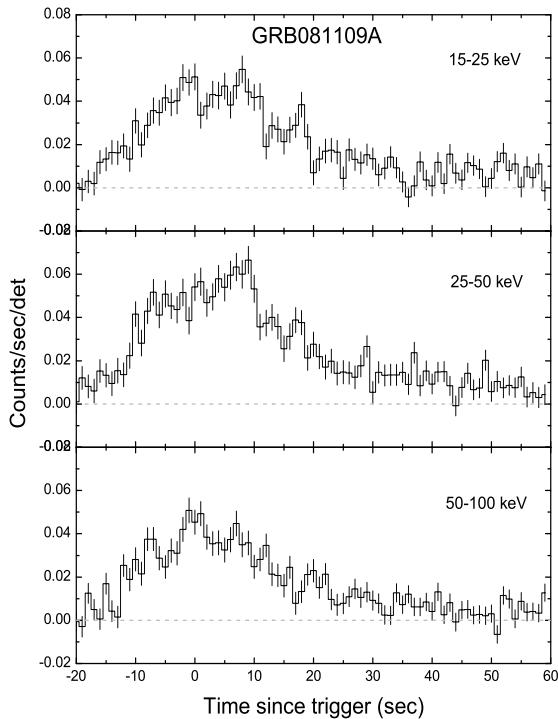


Figure 1. The prompt BAT lightcurves of GRB 081109A in 15-25, 25-50, 50-100 keV with 1 s binning. Spectral lags between different energy bands cannot be well measured for this event due to relatively low signal-to-noise.

to the fitted model. We also considered the most recent calibration and exposure maps. Fig. 2 shows the 0.3-10 keV X-ray lightcurve, which can be well modeled with a doubly broken power-law which is largely equivalent with a broken power-law with a jump transition at ~ 500 s. For a doubly broken power-law, the fitted parameters are: $\alpha_1 = -1.75 \pm 0.04$ ($\chi^2 = 152.4$ for 119), $t_{b1} \sim 310$ s, $\alpha_2 = -0.70 \pm 0.13$ ($\chi^2 = 13.7$ for 18), $t_{b2} \sim 2.9 \times 10^3$ s, $\alpha_3 = -1.24 \pm 0.03$ ($\chi^2 = 38.9$ for 54). The spectral measurements for the above first and third segments are shown in Fig. 3. The spectral power-law indices are $\beta_1 = -0.74 \pm 0.05$, $\beta_3 = -1.27 \pm 0.10$, and β_2 is in the middle of the above two.

The *Swift* Ultraviolet and Optical Telescope (UVOT) began observing at ~ 150 s after the trigger and found no optical counterpart down to ~ 18 mag (Immler et al. 2008). Ground-based REM began observing ~ 52 s after the trigger and found an optical source with $H = 15.47 \pm 0.26$ and $K = 14.51 \pm 0.27$ (D’Avanzo et al. 2008). The object subsequently brightened, reaching $K = 14.27 \pm 0.16$ at ~ 1123 s after the trigger. Ground-based GROND started observation $\sim 6.2 \times 10^4$ s after the trigger, giving a redshift limit of $z < 3.5$ and a best fit of intrinsic extinction of A_v between 0.6 and 1.2 (Clemens, Kruehler, & Greiner 2008). As such, the (published) UV-optical data of GRB 081109A are far from enough to shed light on the medium transition issue apart from the X-ray data, thus they are not taken into account in the following analysis.

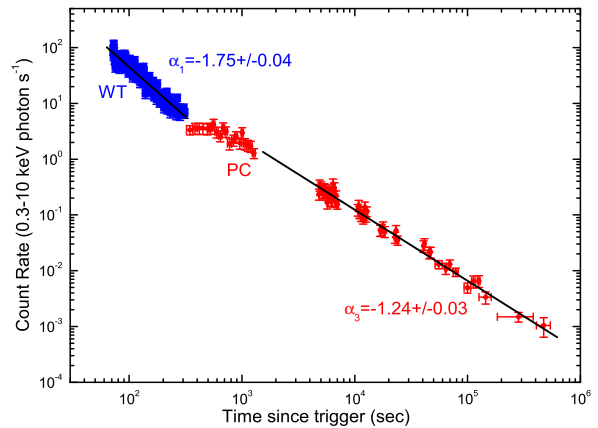


Figure 2. The X-ray afterglow lightcurve of GRB 081109A in 0.3-10 keV. Also marked are the fitting temporal indices for the WT and late PC segments of the lightcurve.

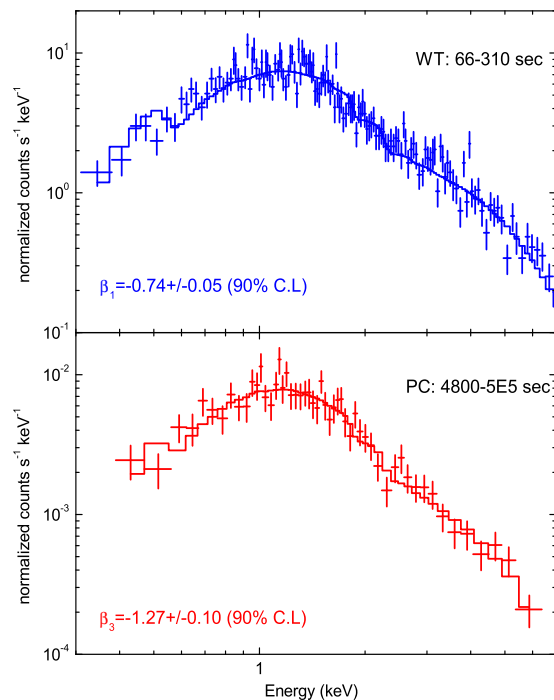


Figure 3. The spectra of the WT and late PC segments of the X-ray afterglow of GRB 081109A. An absorbed power-law fitting is adopted. Also marked are the fitting spectral indices respectively.

3.2 Analytical investigation of the X-ray afterglow

For $t < t_{b1}$, the temporal index $\alpha_1 = -1.75 \pm 0.04$ and the spectral index $\beta_1 = -0.74 \pm 0.05$ are related by $\alpha - 3\beta/2 \approx -0.5$, being consistent with the forward-shock emission in the WIND medium as long as $\nu_m < \nu_X < \nu_c$. For $t > t_{b2}$, the temporal index $\alpha_3 = -1.24 \pm 0.03$ and the spectral index $\beta_3 = -1.27 \pm 0.10$ are related by $\alpha - 3\beta/2 \sim 0.5$, suggesting that the medium can be either WIND or ISM given $\nu_X > \max\{\nu_m, \nu_c\}$ (e.g., Zhang & Mészáros 2004). If the WIND scenario holds from the very beginning, we have $\nu_c(t_{b2}) > \nu_c(t_{b1}) > \nu_X$ because of $\nu_c \propto t^{1/2}$. One can, of course, assume that the wind density or ϵ_B , the fraction of the shock energy given to the magnetic field, changed abruptly and then get a $\nu_c(t_{b2}) \ll \nu_c(t_{b1})$. But such a treatment is lack of solid physical background and is thus unlikely.

On the other hand, if the WIND-ISM medium transition happens at $t \sim t_{b1}$, then the lightcurve due to the forward shock emission will become flattened by a factor of $t^{1/2}$, roughly consistent with the data (note that α_2 is only poorly constrained). In this scenario, the steepening at $t \geq t_{b2}$ implies that $\nu_c(t_{b2}) > \nu_X$. Below we present our quantitative estimates.

According to the closure relation, for $\nu_m < \nu_X < \nu_c$ in the WIND scenario, $\alpha_1 = \frac{1-3p}{4}$ and $\beta_1 = -\frac{p-1}{2}$ hold; for $\nu_X > \max\{\nu_m, \nu_c\}$ in the ISM scenario, $\alpha_3 = \frac{2-3p}{4}$ and $\beta_3 = -\frac{p}{2}$ hold. We found $p = 2.5$ fits the temporal and spectral index fairly well for both segments before and after $t \sim t_{b1}$.

In a free wind medium, we have (e.g., Chevalier & Li 2000):

$$F_{\nu, \max} = 0.23 \text{ Jy } D_{L,28.34}^{-2} \epsilon_{B,-2}^{1/2} E_{k,53}^{1/2} A_* t_{d,-3}^{-1/2}, \quad (1)$$

$$\nu_m = 1.8 \times 10^{16} \text{ Hz } C_p^2 \left(\frac{1+z}{2}\right)^{1/2} \epsilon_{e,-1}^2 \epsilon_{B,-2}^{1/2} E_{k,53}^{1/2} t_{d,-3}^{-3/2}, \quad (2)$$

$$\nu_c = 1.1 \times 10^{13} \text{ Hz } \left(\frac{1+z}{2}\right)^{-3/2} \epsilon_{B,-2}^{-3/2} E_{k,53}^{1/2} A_*^{-2} t_{d,-3}^{1/2}. \quad (3)$$

Here, ϵ_e, ϵ_B is the electron and magnet energy partition. E_k is isotropic equivalent energy. A_* is a density scale for wind, so that wind density at r from center is $\rho = 5 \times 10^{11} A_* r^{-2} \text{ g cm}^{-3}$. n is the density of ISM-like medium. z, D_L is the redshift and the luminosity distance of the GRB. t_d is the time in days since trigger in observation frame. $C_p \equiv 13(p-1)/[3(p-1)]$.

In the ISM, we have (e.g., Sari, Piran, & Narayan 1998):

$$F_{\nu, \max} = 6.6 \text{ mJy } \left(\frac{1+z}{2}\right) D_{L,28.34}^{-2} \epsilon_{B,-2}^{1/2} E_{k,53}^{1/2} n_0^{1/2}, \quad (4)$$

$$\nu_m = 2.4 \times 10^{16} \text{ Hz } C_p^2 \left(\frac{1+z}{2}\right)^{1/2} \epsilon_{e,-1}^2 \epsilon_{B,-2}^{1/2} E_{k,53}^{1/2} t_{d,-3}^{-3/2}, \quad (5)$$

$$\nu_c = 4.4 \times 10^{16} \text{ Hz } \left(\frac{1+z}{2}\right)^{-1/2} \epsilon_{B,-2}^{-3/2} E_{k,53}^{-1/2} n_0^{-1} t_{d,-3}^{-1/2}. \quad (6)$$

In the below analysis we assume that the parameters p, ϵ_e , and ϵ_B are unchanged but the medium are changed from a free wind to ISM.

In our model, $\nu_m < 0.3 \text{ keV}$ and $\nu_c > 10 \text{ keV}$ at 65.6 seconds and $F_{0.3 \text{ keV}} \sim 2.6 \times 10^{-3} \text{ Jy}$. So we have

$$\epsilon_{e,-1}^4 \epsilon_{B,-2} E_{k,53} < 3 \quad (\nu_m < 0.3 \text{ keV}), \quad (7)$$

$$\epsilon_{B,-2}^{3/4} E_{k,53}^{-1/4} A_* < 0.002 \quad (\nu_c > 10 \text{ keV}), \quad (8)$$

$$\epsilon_{e,-1}^{3/2} \epsilon_{B,-2}^{7/8} E_{k,53}^{7/8} A_*^{1/2} \sim 0.02. \quad (9)$$

At $t \sim t_{b2} \sim 2900 \text{ s}$, our model suggests that ν_m and $\nu_c < 0.3 \text{ keV}$, and $F_{0.3 \text{ keV}} \sim 5.7 \times 10^{-5} \text{ Jy}$:

$$\epsilon_{e,-1}^4 \epsilon_{B,-2} E_{k,53} < 8 \times 10^4 \quad (\nu_m < 0.3 \text{ keV}), \quad (10)$$

$$\epsilon_{B,-2}^3 E_{k,53} n_0^2 > 0.01 \quad (\nu_c < 0.3 \text{ keV}), \quad (11)$$

$$\epsilon_{e,-1}^{3/2} \epsilon_{B,-2}^{1/8} E_{k,53}^{9/8} \sim 1.4. \quad (12)$$

Considering the parameters in reasonable region: $\{\epsilon_e, \epsilon_B\} \in [10^{-6} - 1/3]$, $\{A_*, n_0\} \in [10^{-3} - 10^3]$, $E_k \in [10^{52} - 10^{55}] \text{ erg}$. The possible range for these parameters in Eqs.(7-12) is:

$$\begin{aligned} \epsilon_e &\in [0.004 - 0.2], \\ \epsilon_B &\in [0.001 - 0.016], \\ A_* &\in [0.001 - 0.06], \\ n_0 &\in [0.02 - 1000] \text{ cm}^{-3}, \\ E_k &\in [6 \times 10^{52} - 10^{55}] \text{ erg}. \end{aligned}$$

In the termination shock model, the crossing time is estimated by Chevalier, Li, & Fransson (2004)

$$t(R_t) = 1.5 \text{ h } \left(\frac{1+z}{2}\right) E_{k,53}^{-1} A_{*,-1}^2 n_0^{-1} \sim 380 \text{ s}, \quad (13)$$

i.e.,

$$E_{k,53}^{-1} A_{*,-1}^2 n_0^{-1} \sim 0.07. \quad (14)$$

For this particular burst, considering the additional Eq.(14) there is no solution for Eqs.(7-12). We investigate two possibilities. First, the jet parameters are changed when the jet cross the termination shock. Same assumption has been made for GRB050904 (Gendre et al. 2007) and GRB050319 (Kamble et al. 2007). The physical reason is that the ISM-like medium has been heated by the termination reverse shock and then may be higher magnetized. In our modeling ϵ_B in the ISM-like medium is needed to be ~ 10 times to that in WIND.

Second, the jet parameters are unchanged when the jet cross the termination shock, but a higher density jump through the shock. It requests the density jump at least be 40 times to satisfy the observation. We adopt the first assumption in the following numerical fit.

3.3 Numerical fit of the X-ray afterglow

The code used here to fit the X-ray light curves has been developed by Yan, Wei & Fan (2007), with small changes to adapt a density variation in surrounding medium. Assuming a termination shock, we find out that the observation data can be reasonably reproduced with the following parameters (see Fig. 4): the outflow isotropic energy $E_k = 3.0 \times 10^{53} \text{ erg}$ with a initial Lorentz factor $\gamma_0 = 2000$, the WIND density parameter $A_* = 0.01$, the ISM-like medium density $n = 0.1$, the transition radius $R_t = 3.3 \times 10^{17} \text{ cm}$, $\epsilon_e = 0.1$ and $p = 2.5$ in both WIND and ISM-like medium, but the fraction of shock energy given to magnetic field (ϵ_B) changes from 0.0004

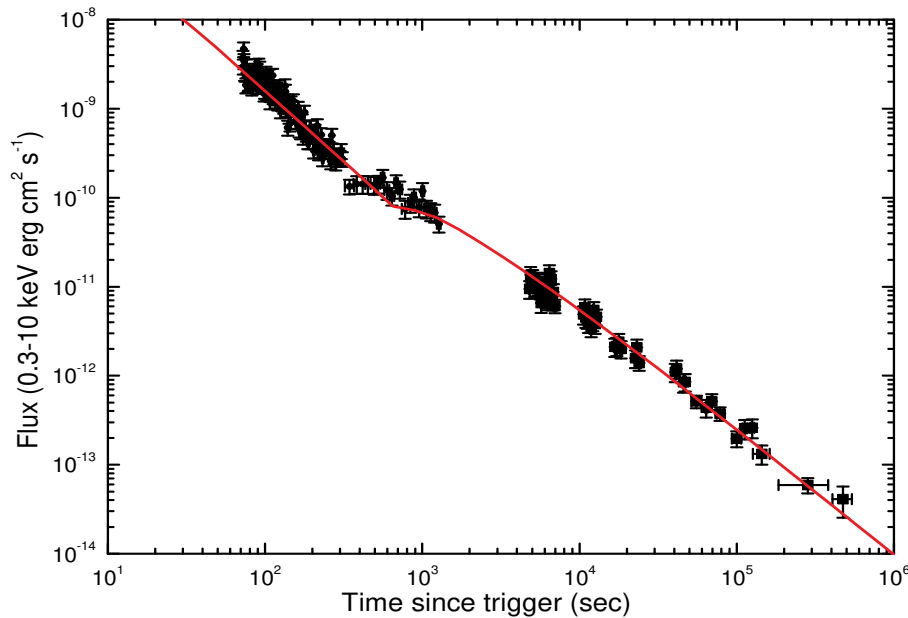


Figure 4. Numerical fit to the afterglow of GRB081109A. The crosses are the observations and the solid line is the fitting. The individual fitting parameters are presented in Section 3.3.

in WIND to 0.002 in ISM-like medium. The source is assumed to be at a redshift $z = 1$.

The X-ray observation lasted to about 470000 seconds. In our numerical fit the jet front reached a radius $\sim 1.87 \times 10^{18}$ cm at that time. The total swept circumburst medium mass is $M \sim \frac{4}{3}\pi R^3 n m_p = 4.6 \times 10^{30}$ g $\sim 2.3 \times 10^{-3} M_\odot$. The total wind mass ejected by the progenitor star in its Wolf-Rayet stage is about $M_w = 0.01 M_\odot \left(\frac{\dot{M}}{10^{-7} M_\odot \text{ year}^{-1}} \frac{T}{10^5 \text{ year}} \right)$. So at the end of observation, the GRB outflow was still in the shocked wind material ejected in the Wolf-Rayet stage, which is suggested as the stellar-wind bubbles with an approximately constant density (Weaver et al. 1977). It is a little earlier than observing the density jump, which causes by the jet front goes into the supergiant shell.

4 CONCLUSION AND DISCUSSION

Observationally the wind signature is not clearly present in a good fraction of GRB afterglows (even for some bursts associated with bright supernovae, see Fan (2008) and the references therein), which may indicate that GRB outflows expand into the wind bubble rather than the ideal free stellar wind. As shown in Section 2 of this work, in some cases the X-ray afterglow data could shed light on this topic. Therefore the X-ray afterglow observation since the early time is required to trace the profile of the circumburst medium. However, in many *Swift* GRB cases the early X-ray afterglow deviate from the standard afterglow model significantly (Nousek et al. 2006; Zhang et al. 2006). For instance, the prolonged activity of GRB central engines would generate energetic X-ray flares that have outshone the regular forward shock emission (e.g., Fan & Wei 2005; Zhang et al. 2006; Nousek et al.

2006). Fortunately, in GRB 081109A there is no flare accompanying the early X-ray afterglow. The temporal and spectral evolutions of the X-ray afterglow imply a medium transition at the radius $R_t \sim 3 \times 10^{17}$ cm (see Section 3). Such a small R_t implies a small wind parameter A_* and a large p/k since

$$R_t = 5.7 \times 10^{17} \left(\frac{v_w}{10^3 \text{ km s}^{-1}} \right) \left(\frac{p/k}{10^6 \text{ cm}^3 \text{ K}} \right)^{-1/2} A_{*, -2}^{1/2} \text{ cm},$$

where p is the pressure in the shocked wind and k is the Boltzmann constant (Chevalier, Li, & Fransson 2004). Indeed the A_* is found to be at the order of 10^{-2} in our numerical fit. GRB 081109A provides more evidence that long GRBs are surrounded by the wind bubble structure, and thus that GRB outflows undergo the WIND-ISM medium transition.

To secure the WIND scenario identification for the early afterglows, it may be necessary to investigate the rise behavior of the very early afterglow lightcurves. This is particularly the case if the reverse shock optical emission is very weak. As shown in Jin & Fan (2007) and Xue et al. (2009), in the WIND scenario the very early optical rise is usually not expected to be faster than $t^{1/2}$ while in the ISM scenario the rise can be faster than t^2 . Therefore the fast $\sim t^3$ -like rise in the early optical/infrared/X-ray afterglows of GRB 060418, GRB 060607A (Molinari et al. 2007), GRB 060801, GRB 060926, GRB 080319C, and GRB 080413B (Xue et al. 2009) rules out the wind medium for $R > 10^{16}$ cm. Thus the absence of the wind signature in some GRB afterglows is still a puzzle. One possible solution is that the mass loss rate due to the stellar wind before massive stars collapse is not a constant and might be much lower than previously assumed.

ACKNOWLEDGMENTS

This work is supported by the National Science Foundation (grants 10673034 and 10621303) and National Basic Research Program (973 programs 2007CB815404 and 2009CB824800) of China. DX is at the Dark Cosmology Centre funded by Danish National Research Foundation. YZF is also supported by Danish National Research Foundation and by Chinese Academy of Sciences.

REFERENCES

- Chevalier, R. A., Li, Z. Y., 2000, *ApJ*, 536, 195
 Chevalier, R. A., Li, Z. Y., Fransson, C., 2004, *ApJ*, 606, 369
 Clemens, C., Kruehler, T., Greiner, J., 2008, *GCN Circ.*, 8515
 Covino, S. et al., 2009, *GCN Circ.*, 8763
 D'Avanzo, P. et al., 2008, *GCN Circ.*, 8501
 Dai, Z. G., Wu, X. F., 2003, *ApJ*, 591, L21
 Eichler, D., Livio, M., Piran, T., Schramm, D. N., 1989, *Nat*, 340, 126
 Fan Y. Z., 2008, *MNRAS*, 389, 1306
 Fan Y. Z., Wei D. M., 2005, *MNRAS*, 364, L42
 Gendre, B. et al., 2007, *A&A*, 462, 565
 Immler, S. et al., 2008, *GCN Circ.*, 8500
 Jin Z. P., Fan Y. Z., 2007, *MNRAS*, 378, 1043
 Kamble, A., Resmi, L., Misra, K., 2007, *ApJ*, 664, L5
 Klotz, A. et al., 2009, *GCN Circ.*, 8764
 Malesani, D. et al., 2009, *GCN Circ.*, 8780
 Mészáros, P., 2002, *ARA&A*, 40, 137
 Molinari, E. et al., 2007, *A&A*, 469, L13
 Nakar, E., 2007, *Phys. Rep.*, 442, 166
 Narayan, R., Paczyński, B., Piran, T., 1992, *ApJ*, 395, L83
 Nousek, J. A. et al., 2006, *ApJ*, 642, 389
 Panaitescu, A., Kumar, P., 2002, *ApJ*, 571, 779
 Piran, T., 1999, *Phys. Rep.*, 314, 575
 Ramirez-Ruiz, E., Dray, L. M., Madau, P., Tout, C. A., 2001, *MNRAS*, 327, 829
 Sari, R., Piran, T., Narayan, R., 1998, *ApJ*, 497, L17
 van Marle, A. J., Langer, N., Achterberg, A., Garcia-Segura, G., 2006, *A&A*, 460, 105
 van Marle, A. J., Langer, N., García-Segura, G., 2007, *A&A*, 469, 941
 von Kienlin, A., 2008, *GCN Circ.* 8505
 Weaver, R., McCray, R., Castor, J., Shapiro, P., Moore, R., 1977, *ApJ*, 218, 377
 Wijers, R. A. M. J., 2001, *Gamma-Ray Bursts in the Afterglow Era: Proceedings of the International Workshop Held in Rome, Italy, 17-20 October 2000, ESO ASTROPHYSICS SYMPOSIUM*. Edited by E. Costa, F. Frontera, and J. Hjorth. Springer-Verlag, 306
 Woosley, S., 1993, *ApJ*, 405, 273
 Xue, R. R., Fan, Y. Z., Wei, D. M., 2009, *A&A*, in press, preprint (astro-ph/0902.2613)
 Yan, T., Wei, D. M., Fan, Y. Z., 2007, *Chin. J. Astron. Astrophys.*, 7, 777
 Zhang, B. et al. 2006, *ApJ*, 642, 354
 Zhang, B., Mészáros, P., 2004, *IJMPA*, 19, 2385